# Roman Core Community Survey White Papers

# *A wide-area extension to the Roman HLIS for multiwavelength galaxy cluster science*

**Roman Core Community Survey:** High Latitude Wide Area Survey (Imaging)

**Scientific Categories:** Large scale structure of the universe

**Submitting Author**: Anja von der Linden (Stony Brook University, anja.vonderlinden@stonybrook.edu)

**Co-authors/Endorsers**: Steven Allen (Stanford), Camille Avestruz (University of Michigan), Lucie Baumont (CEA Paris-Saclay), Bradford Benson (University of Chicago, Fermilab), Simon Birrer (Stony Brook University), Lindsey Bleem (Argonne National Laboratory), Sebastian Bocquet (LMU Munich), Maruša Bradač (University of Ljubljana), Esra Bulbul (MPE), Céline Combet (IN2P3/LPSC, Grenoble), Matteo Costanzi (University of Trieste), Ian Dell'Antonio (Brown), Mariano Domínguez (IATE-OAC-UNC), Cyrille Doux (IN2P3/LPSC, Grenoble), Tim Eifler (UArizona), Shenming Fu (NOIRLab), Matt Hilton (Wits University), Patrick Kelly (University of Minnesota), Elisabeth Krause (UArizona), Adam Mantz (Stanford), Michael McDonald (MIT), Vivian Miranda (Stony Brook University), Marina Ricci (APC/IN2P3, Paris), Stella Seitz (LMU, Munich), Tae-hyeon Shin (Stony Brook University), Adam Wright (Milwaukee School of Engineering)

**Abstract:**
We advocate for a wide-area extension of the Roman High Latitude Imaging Survey (HLIS) covering much of the Rubin/LSST extragalactic area to maximize the scientific potential of galaxy clusters. Roman will be one of the most powerful instruments for galaxy cluster weak lensing measurements in the next decade, owing to its space-based resolution, large collecting area, and near-infrared sensitivity. Current and future experiments at X-ray and millimeter wavelengths are in the process of, or planning to, survey much of the Rubin/LSST extragalactic sky, identifying clusters by their dominant baryonic mass component (the hot intracluster gas via its X-ray emission / Sunyaev-Z'eldovich [SZ] decrement) out to high redshifts. A wide-area extension of the Roman HLIS will thus significantly increase the number of the most massive clusters ($\gtrsim 10^{15}\mathrm{M}_{\odot}$) with high-quality, multi-wavelength data including Rubin+Roman weak (and strong) lensing. The most massive clusters open up a rich discovery space for astrophysics and cosmology, from studying the (dark matter) mass distribution in extreme mergers, galaxy evolution in the densest environments, to identifying the most powerful strong lenses to probe the high-redshift Universe. For cluster cosmology, compared to the reference HLIS, the wide-area survey offers the compelling trade-off to limit the selection to a higher, more conservative target mass threshold, where the systematics related to the mass-observable relation can be much better constrained through the incorporation of X-ray and SZ information, and higher weak-lensing signal-to-noise ratios per cluster. Altogether, a wide-area Roman survey would build a powerful legacy dataset for cluster science.

# 1 Introduction

Clusters of galaxies are key science drivers for the Roman High Latitude Imaging Survey (HLIS; Spergel et al., 2015). For cosmology, measurements of the cluster mass function and its evolution can in principle deliver very powerful constraints, if systematics related to cluster mass measurements can be controlled (Dodelson et al., 2016). Clusters are one of the prime laboratories for dark matter, where the distribution of matter can be directly inferred with weak and strong lensing. As the highest density cosmological environments, they provide important insights into the physics driving galaxy evolution. Moreover, they are powerful gravitational telescopes, enabling the study of high-redshift objects that would otherwise be too faint to observe.

However, the reference High Latitude Wide Area Survey (HLWAS) covers only about $\sim 5\%$ of the full sky. Due to the exponential cut-off of the halo mass function (Fig. 1), truly massive clusters ($\gtrsim 10^{15}\mathrm{M}_{\odot}$) are rare, and will therefore be largely missing from the HLWAS. These most massive clusters are disproportionately important for cosmology and astrophysics. Not only do they carry significant cosmological constraining power, they also open up vast discovery space for astrophysics and dark matter under extreme conditions, as evidenced e.g. by the posterchild cluster for dark matter studies, the Bullet Cluster (Clowe et al., 2006a). Moreover, through strong lensing they are the most powerful gravitational telescopes, allowing us to peer deeper into the high-redshift Universe than otherwise possible. A wide-area extension of the HLIS within the Rubin/LSST extragalactic survey area ($\sim 17,000$ sq. deg.) in the W-band (F146W, approximately $0.93 - 2.00\mu m$), as has been proposed in other white papers, would increase the number of massive clusters with the homogeneous Rubin/LSST and Roman imaging by a factor of $\sim 10$. It would optimally complement not just Rubin/LSST, but also the all-sky eROSITA X-ray survey, and the large-area CMB surveys e.g. ACT, SO, and CMB-S4. Specifically, the community would gain near-infrared, space-based resolution images deep enough to match the Rubin/LSST imaging of *all* massive clusters in the southern extragalactic sky, including immediate high-quality, multi-wavelength data to identify and study the rarest, most extreme objects in the Universe, and conduct multi-wavelength cosmology analyses anchored by Rubin+Roman weak lensing.

We here discuss the benefits of such a wide-area extension for science with galaxy clusters. We pay particular attention to cluster weak lensing, owing to Roman's formidable weak-lensing capabilities especially for clusters due to its depth and space-based resolution. Eifler et al. (2021) showed that a wide-area W-band survey would detect 95% of the objects in the LSST 10-year gold sample catalog in just 5 months observing time. While Euclid will provide space-based imaging for these clusters, as well, such a Roman W-band survey would be deeper, and would reach higher-redshift background sources - both of which makes this particularly compelling for cluster weak lensing. As other white papers, we advocate for a *wide* survey tier in addition to a *medium* tier that closely resembles the reference survey with a reduced survey area of $\sim 1000$ sq. deg. in four Roman bands. The latter would serve as a calibration sample for photo-z's and PSF systematics.

We note that with high likelihood, a subset of massive clusters not in the reference survey footprint will be the targets of Guest Observer programs with Roman (and JWST and Hubble) based upon identification in other surveys, as has also been – very successfully – the case with Hubble. However, this means that there will be significant delay in acquiring these data, the data will be quite heterogeneous, and will not cover the full radial extent to which the ("2-halo") weak-lensing signal can be measured. Given the nature of the proposed survey extension in a single-band, the proposal here does not preclude follow-up targeted observations in more bands and in greater depths. Rather, it will serve to identify the best targets, e.g. the most extreme clusters, and the clusters with the highest strong-lensing cross sections.

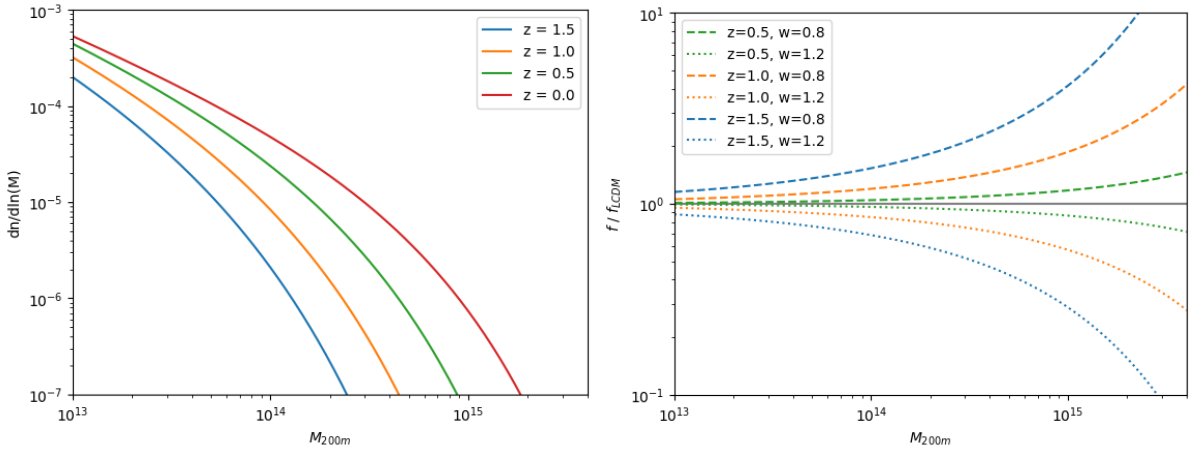


Figure 1: The evolution of the halo mass function (HMF), and its dependence on cosmology. The left panel shows the HMF (in a ΛCDM cosmology) at four different redshifts - the most massive clusters are rare, and need large survey volumes to be found. The right panel shows the ratio of the HMF in two $w$CDM cosmologies ($w = -0.8$ and $w = -1.2$) to the reference $w = -1.0$ case. The impact of dark energy is largest for the most massive clusters. The HMF is computed from the Tinker et al. (2008) fitting function; the figure was made using the COLOSSUS package by Diemer (2018).

## 2 Cluster weak lensing

Roman will arguably be the most powerful instrument for cluster weak lensing - especially at high redshifts - in the next decade, due to its space-based resolution and high sensitivity in the near-infrared. Cluster weak lensing plays a key role in cluster cosmology, but also in dark matter studies through mass mapping in disassociative mergers and measurements of cluster density profiles. Compared to LSST-only (or LSST+Euclid) imaging, the Roman W-band imaging would significantly improve the statistical and systematic uncertainties of cluster weak-lensing measurements via these aspects:

### 2.1 Deblending

At LSST depth, more than half of all objects are expected to be blended (LSST Dark Energy Science Collaboration, 2012; Bosch et al., 2018), and roughly 10-15% are expected to be unrecognized blends (i.e. where a ground-based detection corresponds to two or more "true" objects; Dawson et al., 2016; Troxel et al., 2023). These numbers are even higher in the fields of galaxy clusters, which are overdense extragalactic fields by definition. Clusters therefore are arguably the weak-lensing application that can gain the most from the addition of space-based resolution. Since typical Euclid imaging does not reach the depth of LSST imaging, the W-band survey would optimally deliver deblending information for an LSST+Roman(+Euclid) catalog. In return, the existing LSST colors would potentially improve the deblending through multi-band information (Melchior et al., 2018).

### 2.2 Photometric redshifts

Compared to cosmic shear, cluster weak lensing has the additional challenge of contamination of the source galaxy sample by misidentified cluster galaxies. Since cluster galaxies carry zero shear, including them in the source sample dilutes the signal. The addition of W-band photometry to LSST photometry broadens the wavelength coverage, thereby improving photometric redshift estimates. While the gain is only modest

compared to the four-band imaging in the reference survey, the medium tier imaging can be used to calibrate photo-z systematics for the wide survey. Also note that the Roman W-band imaging extends the wavelength coverage into the NIR, which the Euclid-VIS imaging does not (Euclid does, of course, add NIR imaging, but the depth is comparatively shallow).

### 2.3 Redshift reach

The addition of Roman W-band imaging will particularly boost the number of usable source galaxies at $z \gtrsim 1$. Its greatest impact will therefore be for clusters at $z \gtrsim 0.8$, whose angular size on the sky is small, and for which the number density of background sources selected in the optical (including by Euclid-VIS) is small. High-redshift clusters hold significant cosmological constraining power (Fig. 1), given the sensitivity of cluster formation to dark energy and the relatively recent transition from a matter dominated regime.

### 2.4 Identification of the central galaxy

Current optical cluster samples misidentify the central cluster galaxy in about $\sim 30\%$ of clusters (Zhang et al., 2019; Bleem et al., 2020), leading to errors in the galaxy richness measurement and uncertainty in the weak-lensing mass calibration. A promising method to identify the central galaxies in deeper imaging than current surveys uses the outer stellar envelopes of massive galaxies – essentially, the galaxy with the most prominent outer envelope is the most likely central galaxy (Huang et al., 2022). The outer envelopes (just as the Intracluster Light, ICL) consists of old stellar populations; therefore the peak emission is in the near-infrared, which makes this application an excellent case for Roman W-band imaging. This is particularly the case for increasing cluster redshifts, where much of the emission will shift out of the deepest LSST imaging. Since this a low-surface brightness measurement, care will need to be taken in choosing dithering positions and roll angles to mitigate the impact of reflections in the optical path (Montes et al., 2023). In addition, the morphology of the central galaxy indicates the merger history and triaxiality of the cluster (Herbonnet et al., 2022), and the central galaxy's offset from the cluster center can constrain the dark matter self-interaction cross section (Kim et al., 2017); an improvement on the identification of the central galaxy will strengthen these measurements.

### 2.5 Signal-to-noise per cluster

Cluster cosmology with optically selected cluster samples so far has used stacked weak-lensing measurements for the mass calibration (e.g. McClintock et al., 2019), owing to the large number of cluster detections, and the low typical signal-to-noise per cluster. The latter is both due to the typically low mass of optically selected clusters, as well as the low number density of source galaxies in the relatively shallow, ground-based survey imaging available so far. In contrast, state-of-the-art cluster cosmology from X-ray and SZ samples has used hierarchical modeling with individual weak-lensing masses (Mantz et al., 2015; Bocquet et al., 2019). Hierarchical modeling has the advantage that it can optimally use all the data available for each cluster, avoiding the loss of per-cluster information inherent to stacking techniques. Moreover, it simultaneously and self-consistently constrains both cosmology and the parameters of the mass-observable relation (Fig. 3) from the data itself, rather than requiring external calibration steps. Hierarchical models can in principle be applied to large ensembles of low-SNR data, but the benefits are largest when each measurement is a confident detection.

At face value, the expected increase in the number density of lensing source galaxies (for the full survey area) is modest: $\sim$ 27 gal./sq. arcmin for LSST-Y10 vs. $\sim$ 41 gal./sq. arcmin for LSST+HLS-Wide.

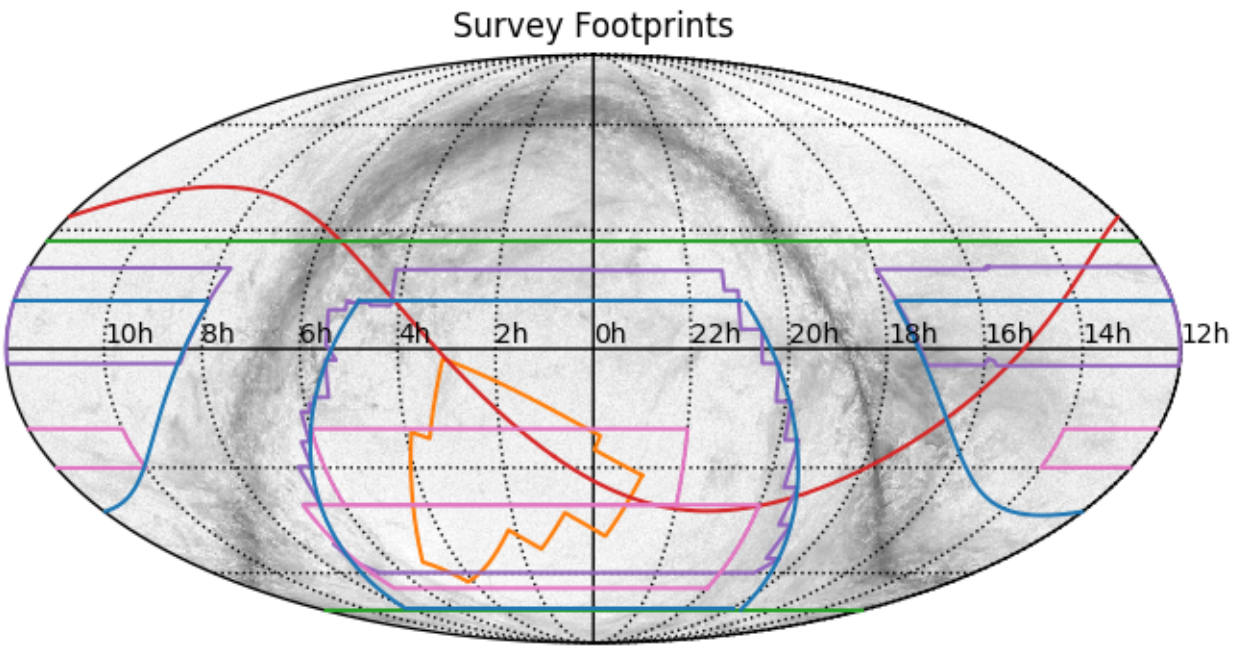


Figure 2: An all-sky overview of the survey footprints of several surveys discussed in the paper. The figure is in equatorial coordinates, with right ascension labels. The background greyscale is the Planck dust map. The orange outline shows the footprint of the reference HLIS. In blue, we show an approximation to the LSST extragalactic survey area (note that the LSST survey strategy has not been finalized), assuming a declination range of -72 to 12 degrees, and an exclusion around the galactic plane of $\pm 12$ degrees. The red line denotes the eROSITA data split into a German (southern) and a Russian (northern) hemisphere. In green, we show the sky area reachable by SZ telescopes in the Atacama desert observing to 40 degrees elevation - both the Simons Observatory and CMB-S4 survey footprints are still to be finalized, as well. The purple and pink outlines show the footprints of existing high-resolution SZ cluster samples: ACT DR5 is shown in purple, and SPT-SZ and SPT-ECS in pink.

However, these numbers neglect that deep, ground-based weak-lensing measurement at small cluster radii ($\lesssim 500$ kpc) are significantly hampered by the higher density of galaxies and thus increased blending. The Roman data will allow fitting to smaller radii, thereby including the regions where the weak-lensing signal is strongest. In addition, the NIR-selection will shift the redshift distribution of source galaxies to higher redshifts, boosting the number density of background galaxies, which is particularly beneficial to high-redshift clusters. Therefore, the overall boost in signal-to-noise will be much greater than the square root of the ratio of the number densities.

## 3 Synergy with X-ray and SZ surveys

On-going and planned SZ and X-ray surveys are in the process of identifying large samples of clusters, selected by their dominant baryonic component – the intracluster gas – out to high redshifts (Fig. 3). They have already discovered some of the most extreme objects in the Universe, such as the Phoenix cluster, an SZ-discovered, exceptionally X-ray-bright cluster with a run-away cooling flow (McDonald et al., 2012) and El Gordo, an extremely massive high-redshift merging cluster (Menanteau et al., 2012). The cluster samples identified by these surveys lay the ground-work for precision cluster cosmology with gas-selected clusters. However, for both astrophysics and cosmology, X-ray and SZ surveys require optical / near-infrared data for cluster confirmation, redshift determination, and weak-lensing mass estimates. All of these will benefit

from the addition of Roman W-band imaging to LSST (and Euclid) imaging. This is especially the case for high-redshift clusters $z \gtrsim 1$, for which even the Euclid data will typically be too shallow for individual weak-lensing mass measurements.

While the initial SPT-SZ and ACT survey areas were comparatively small, SZ surveys are moving towards wide-area, deep coverage of the LSST survey area. ACT DR5 already covers an area of $\approx 13,000$ sq. deg., SPT-3G is in the process of surveying 10,000 sq degrees of the LSST sky, and both Simons Observatory and CMB-S4 plan to observe the full LSST extragalactic sky. Owing to their roughly constant mass limit with redshift, SZ surveys are particularly interesting for selecting high-redshift clusters – which would optimally be matched by Roman data.

In the X-ray band, the eROSITA (extended ROentgen Survey with an Imaging Telescope Array) telescope on board the Russian–German Spectrum Roentgen Gamma mission has completed four of the planned eight sky surveys since its launch in 2019 (Predehl et al., 2021; Sunyaev et al., 2021). The publication rights of the data in the Western Galactic Hemisphere belong to the German eROSITA consortium (eROSITA-DE), and the eROSITA-DE data are being released at a regular cadence (see Brunner et al., 2022). When the planned final depth is reached after the eighth survey is completed, eROSITA is expected to deliver more than 100,000 clusters of galaxies and galaxy groups in a redshift range from 0.01 to 1.5 and a large mass interval from $10^{12}$ $M_{sun}$ to $10^{15}$ $M_{sun}$ (Pillepich et al., 2018; Liu et al., 2022; Bulbul et al., 2022). While eROSITA goes significantly deeper than its predecessor ROSAT, selection by X-rays incurs a strong redshift dependence due to cosmological surface brightness dimming limiting the detection of high redshift clusters (see Fig. 3). However, besides the selection observables (such as count rate), eROSITA can measure X-ray properties for a subset of the clusters, such as (core-excised) luminosity, gas mass, temperature, and the proxy $Y_X$. Gas mass can be measured from just $\sim 500$ X-ray counts, and scales much tighter with cluster mass than the survey observables (X-ray luminosity, SZ significance, optical richness), which makes it an invaluable component of cluster cosmology (Sect. 4). Since at $z \gtrsim 0.5$, gas masses from eROSITA survey data will be possible only for the most massive clusters (Fig. 3), a wide-area Roman survey would optimally complement the multi-wavelength data for these clusters.

The wide-area extension would boost the number of massive clusters with SZ and X-ray measurements, *and* deep, space-based near-infrared imaging from Roman for weak and strong lensing by a factor of $\sim 10$. The resulting sample will probe a larger diversity of objects and extreme environments for galaxy formation, and open the discovery space for the rarest, most unusual objects. It would also enable multi-wavelength cluster cosmology, anchored by Rubin+Roman weak-lensing mass estimates.

# 4 Cluster cosmology

Cosmology with measurements of the cluster mass function and its evolution, as traced by clusters of galaxies, is one of the core goals of the HLIS (Spergel et al., 2015). Cluster cosmology with the reference Roman HLIS survey requires including lower-mass clusters (target mass threshold $\sim 10^{14} M_{\odot}$), but recent work has shown that the selection function and weak-lensing mass estimates of optically selected cluster samples at lower masses are difficult to characterize because of projection and astrophysical effects (DES Collaboration et al., 2020), leading to biases in the inferred cosmology. While these also affect the most massive clusters, the combination of multi-wavelength datasets (esp. SZ and X-rays) significantly boosts our ability to characterize the cluster selection function and the mass-observable relation.

The survey observables by which clusters are identified (galaxy richness, SZ significance, X-ray luminosity) all scale with cluster mass, albeit with large scatter ($\sim 20 - 40\%$; Fig. 3). Because of the steepness of the halo mass function, this means that any cluster sample above some fixed observable limit contains

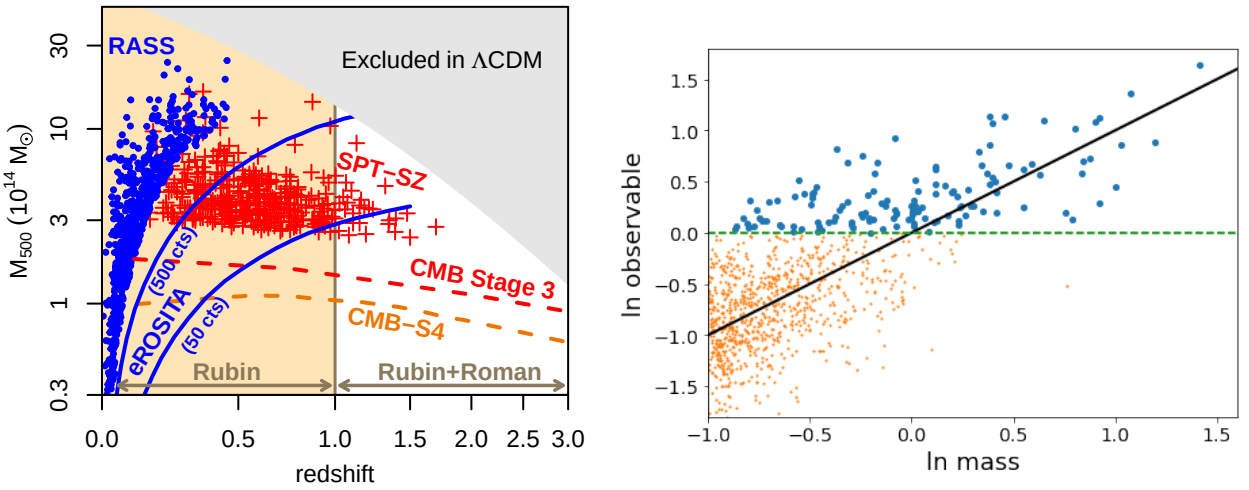


Figure 3: Left: mass limits as function of redshift for X-ray and SZ surveys. Shown are the cluster cosmology catalogs from the ROSAT All-Sky Survey (RASS) and the SPT-SZ survey. For upcoming CMB surveys, the approximate 50% completeness mass limits are shown. For eROSITA, we show two lines for the expected 50% completeness mass limits: the detection limit (50 counts), and the limit for acquiring gas mass measurements (500 counts). Right: an illustration of the scatter in the mass-observable relation on cluster selection. Due to the self-similarity of clusters, the mean relation (black line) between halo mass and observable is generally well approximated as a power-law. However, all survey observables (galaxy richness, X-ray luminosity, and SZ significance), as well as weak-lensing masses, have significant scatter around the mean relation ($\sim 20-40\%$, approximately log-normal). Due to the steepness of the mass function, at any fixed selection threshold in the observable, a large fraction of the detected clusters are lower-mass systems that scatter up. Low-scatter mass proxies such as X-ray gas masses can significantly help to constrain the shape and scatter of the mass-observable relation. The combination of multi-wavelength observables can further aid in modelling the selection function and mass-observable relation.

a significant fraction of clusters below the nominal mass threshold that have "scattered up" (Fig. 3). Similarly, individual weak-lensing have a scatter of $\sim 30\%$ with halo mass. The source of scatter is partly astrophysical, stemming from cluster shape and dynamical stage, age, projection of structure along the line of sight, etc., and is correlated between the different mass proxies: e.g. projection causes both richness and weak-lensing signal to scatter up; at fixed mass, older clusters are expected to be more spherical (Lau et al., 2021), have higher concentration, and higher X-ray temperature and SZ signal (Chen et al., 2019). With multi-wavelength observations (and especially with low-scatter mass proxies such as gas mass [or $Y_X$] from eROSITA), physical models for these sources of scatter could be constructed and constrained. However, at the Roman target mass limit of $\sim 10^{14}\mathrm{M}_\odot$, a large fraction of cluster candidates will not be detected by SZ or X-rays, simply due to the large scatter around the mean scaling relations (Fig. 3). A wide-area survey extension offers a compelling alternative: with a wider area, the same cosmological constraining power can be achieved with a higher target mass threshold, and in particular, the systematics relating to cluster selection and the mass-observable relation can be much better constrained with the availability of multi-wavelength data.

## 5 Strong-lensing discovery space

Within cluster samples, the most massive clusters have the largest strong-lensing cross-sections. Although cluster mergers can increase the caustic surface area significantly, it will always be the most massive systems that provide the richest and best-modeled probes of the high redshift Universe through magnification. While studies of a few systems with JWST have yielded exceptionally rich information on the highest redshift galaxies (Adams et al., 2022), only a very small fraction of the highly magnified space behind massive clus-

ters will be studied by JWST in its lifetime. This is particularly true for the study of lensed transients such as Supernovae (Kelly et al., 2015, 2023a). Cluster-scale lenses can yield months to years long time delays that enable high-precision measurements, as was the case for SN Refsdal which yielded a 1.5% measurement (Kelly et al., 2023b). Only two epochs of imaging would be required for detection of transients. Moreover, models of cluster-scale lenses have different systematic uncertainties from those of galaxy-scale lenses used for current quasar time-delay constraints on the Hubble constant. As each strongly lensed Supernova is an independent test of the scale of the Universe (via time delay), a survey such as the one proposed will provide a complementary test on the same length scale as the lensed quasar time delays, but with negligible uncertainty on the delay itself. Using the wide HLWAS survey as the discovery image for lensed supernovae will allow for efficient targeted followup. This is particularly important for the discovery of strongly lensed Type Ia supernovae, where the both time delay and lightcurve stretch can be used to constrain $H_o$ and dark energy simultaneously (Qi et al., 2022). Finally, a wide HLWAS has the potential to discover bright microlensing events of individual stars highly magnified by foreground clusters.

The pairing of a large sample of massive clusters with high resolution strong lensing in the center and high S/N weak lensing measurements with the complementary X-ray and SZ measurements also produces a sensitive test of the nature of dark matter via mapping of separation between the baryonic and dark matter components in clusters (Clowe et al., 2006b). The higher resolution reconstruction enabled by the HLWAS survey will improve measurement of the mass substructures of galaxy clusters, particularly in the outskirts where the Roman field of view is critical. The wide HLWAS survey will place constraints on the self interaction cross section smaller than $\sim 0.5$ cm$^2$/g, and a unique constraint on a velocity-dependent cross-section at $v \sim 1000$ km/s (Bhattacharyya et al., 2022).

# References


Adams N. J., et al., 2022, Monthly Notices of the Royal Astronomical Society, 518, 4755

Bhattacharyya S., Adhikari S., Banerjee A., More S., Kumar A., Nadler E. O., Chatterjee S., 2022, ApJ, 932, 30

Bleem L. E., et al., 2020, ApJS, 247, 25

Bocquet S., et al., 2019, ApJ, 878, 55

Bosch J., et al., 2018, PASJ, 70, S5

Brunner H., et al., 2022, A&A, 661, A1

Bulbul E., et al., 2022, A&A, 661, A10

Chen H., Avestruz C., Kravtsov A. V., Lau E. T., Nagai D., 2019, MNRAS, 490, 2380

Clowe D., Bradač M., Gonzalez A. H., Markevitch M., Randall S. W., Jones C., Zaritsky D., 2006a, ApJ, 648, L109

Clowe D., Bradač M., Gonzalez A. H., Markevitch M., Randall S. W., Jones C., Zaritsky D., 2006b, The Astrophysical Journal, 648, L109

DES Collaboration et al., 2020, Phys. Rev. D, 102, 023509

Dawson W. A., Schneider M. D., Tyson J. A., Jee M. J., 2016, ApJ, 816, 11

Diemer B., 2018, ApJS, 239, 35

Dodelson S., Heitmann K., Hirata C., Honscheid K., Roodman A., Seljak U., Slosar A., Trodden M., 2016, arXiv e-prints, p. arXiv:1604.07626

Eifler T., et al., 2021, MNRAS, 507, 1514

Herbonnet R., et al., 2022, MNRAS, 513, 2178

Huang S., et al., 2022, MNRAS, 515, 4722

Kelly P. L., et al., 2015, Science, 347, 1123

Kelly P. L., et al., 2023a, Science, 380, abh1322

Kelly P. L., et al., 2023b, ApJ, 948, 93

Kim S. Y., Peter A. H. G., Wittman D., 2017, MNRAS, 469, 1414

LSST Dark Energy Science Collaboration 2012, arXiv:1211.0310,

Lau E. T., Hearin A. P., Nagai D., Cappelluti N., 2021, MNRAS, 500, 1029

Liu A., et al., 2022, A&A, 661, A2

Mantz A. B., et al., 2015, MNRAS, 446, 2205

McClintock T., et al., 2019, MNRAS, 482, 1352

McDonald M., et al., 2012, Nature, 488, 349

Melchior P., Moolekamp F., Jerdee M., Armstrong R., Sun A. L., Bosch J., Lupton R., 2018, Astronomy and Computing, 24, 129

Menanteau F., et al., 2012, ApJ, 748, 7

Montes M., et al., 2023, arXiv e-prints, p. arXiv:2306.09414

Pillepich A., Reiprich T. H., Porciani C., Borm K., Merloni A., 2018, MNRAS, 481, 613

Predehl P., et al., 2021, A&A, 647, A1

Qi J.-Z., Cui Y., Hu W.-H., Zhang J.-F., Cui J.-L., Zhang X., 2022, Physical Review D, 106

Spergel D., et al., 2015, arXiv e-prints, p. arXiv:1503.03757

Sunyaev R., et al., 2021, A&A, 656, A132

Tinker J., Kravtsov A. V., Klypin A., Abazajian K., Warren M., Yepes G., Gottlöber S., Holz D. E., 2008, ApJ, 688, 709

Troxel M. A., et al., 2023, MNRAS, 522, 2801

Zhang Y., et al., 2019, MNRAS, 487, 2578